



OPEN ACCESS

EDITED BY

Joel Fernando Soares Filipe,
University of Milan, Italy

REVIEWED BY

Lan Wang,
University of Minnesota Twin Cities,
United States

Hai Li,
Xi'an Jiaotong University, China

*CORRESPONDENCE

LianXiang Wang
✉ animsci@126.com
Lang Gong
✉ gonglang@scau.edu.cn

†These authors have contributed equally to
this work

RECEIVED 16 October 2024

ACCEPTED 09 January 2025

PUBLISHED 31 January 2025

CITATION

Qiu Y, Li Q, Zhao W, Chang H, Wang J, Gao Q,
Zhou Q, Zhang G, Gong L and Wang L (2025)
Evaluation of the killing effects of UV₂₅₄ light
on common airborne porcine viruses.
Front. Vet. Sci. 12:1512387.
doi: 10.3389/fvets.2025.1512387

COPYRIGHT

© 2025 Qiu, Li, Zhao, Chang, Wang, Gao,
Zhou, Zhang, Gong and Wang. This is an
open-access article distributed under the
terms of the [Creative Commons Attribution
License \(CC BY\)](https://creativecommons.org/licenses/by/4.0/). The use, distribution or
reproduction in other forums is permitted,
provided the original author(s) and the
copyright owner(s) are credited and that the
original publication in this journal is cited, in
accordance with accepted academic
practice. No use, distribution or reproduction
is permitted which does not comply with
these terms.

Evaluation of the killing effects of UV₂₅₄ light on common airborne porcine viruses

YingWu Qiu^{1,2†}, QunHui Li^{2†}, WenKai Zhao², Hao Chang^{1,2},
JunHua Wang³, Qi Gao^{1,4}, Qingfeng Zhou², GuiHong Zhang^{1,4},
Lang Gong^{1,4*} and LianXiang Wang^{2*}

¹Guangdong Provincial Key Laboratory of Zoonosis Prevention and Control, College of Veterinary Medicine, South China Agricultural University, Guangzhou, China, ²Guangdong Provincial Key Laboratory of Livestock and Poultry Health and Environmental Control, Yunfu, China, ³Foshan Comwin Light & Electricity Co., Ltd., Foshan, China, ⁴African Swine Fever Regional Laboratory of China (Guangzhou), Guangzhou, China

UV exposure is a common method of disinfection and sterilization. In the present study, the parallel beam test was performed to collect fluids containing infectious viruses using a parallel beam apparatus after UV₂₅₄ irradiation (0, 0.5, 1, 3, 5, 7, 10, or 20 mJ/cm²). The air sterilization test was performed by irradiating the air in the ducts with UV₂₅₄ light (0, 1, 2, 3, 4, or 6 mJ/cm²) to collect airborne particles containing viruses through the air sterilization equipment. Furthermore, viral inactivation was assessed based on cytopathic effect (CPE) detection and immunofluorescent assays (IFA). Both the CPE and immunofluorescence signal intensity decreased as the UV₂₅₄ dose increased. The UV₂₅₄ doses required to inactivate ASFV (10^{7.75} copies/mL), PRRSV (10^{6.29} copies/mL), and PEDV (10^{7.71} copies/mL) in the water were 3, 1, and 1 mJ/cm², respectively. The UV₂₅₄ dose required to inactivate ASFV (10^{4.06} copies/mL), PRRSV (10^{3.06} copies/mL), and PEDV (10^{4.68} copies/mL) in the air was 1 mJ/cm². This study provides data required for biosecurity prevention and control in swine farms.

KEYWORDS

UV radiation, air disinfection, ASFV, PRRSV, PEDV

1 Introduction

China is the world's largest producer and consumer of pork, producing approximately 53% of the global pork supply (1). Furthermore, pork is the main source of high-quality protein for Chinese residents, with the consumption accounting for 62% of total meat consumption (2). Infectious diseases represent a major constraint to pig production (3). Since the first outbreak of African swine fever (ASF) in China in August 2018, ASF, porcine reproductive and respiratory syndrome (PRRS), and porcine epidemic diarrhea (PED) have emerged as the three most serious viral diseases in Chinese pig farms (4). These diseases are highly transmissible and pathogenic, with rapid mutation of the virulent strains, resulting in abortions in sows, growth delay in fattening pigs, and mass mortality among piglets (5, 6). When these diseases occur on pig farms, it is difficult to achieve decontamination because of the labor and resources required to control the spread of the disease in the herd. Notably, ASF virus (ASFV), PRRS virus (PRRSV), and PED virus (PEDV) can be transmitted through the air, further complicating disease prevention and control efforts in the entire Chinese pig farming industry (7–10).

UV disinfection is one of the most commonly used methods for preventing air-mediated microbial disease transmission because of its low cost, simple installation, ease of maintenance,

and significant effectiveness (11, 12). UV light can inactivate pathogenic microorganisms through several mechanisms, such as the formation of cyclobutane pyrimidine dimers in nucleic acids, which ultimately inhibit transcription and replication (13). In addition, the generation of reactive oxygen species (ROS) results in the oxidation of macromolecules such as lipids, proteins, and carbohydrates inside the cells and leads to cell membrane and cell wall damage (14). Table 1 provides a summary of recent studies on the effectiveness of UV in inactivating various viruses. From these references, we can identify that in addition to the UV dose, important factors affecting UV disinfection include the wavelength of the UV light used, the type of virus, the environmental conditions, and the medium through which UV light is transmitted.

Previous studies have shown that UV disinfection is an effective method to inactivate a wide range of pathogenic microorganisms, including various phages and viruses such as SARS-CoV-2 (15–22). This study aimed to evaluate the inactivating effect of UV₂₅₄ light, a UV-C wavelength, on common airborne porcine viruses, providing critical data for the prevention and control of animal diseases.

2 Materials and methods

2.1 Viruses and cells

ASFV, PRRSV, and PEDV were obtained from the National Regional Laboratory for African Swine Fever (Guangzhou) of South China Agricultural University (Guangzhou, China). Porcine primary alveolar macrophages (PAMs) were isolated from the bronchoalveolar lavage fluid of 4-week-old healthy piglets. Marc-145 and Vero cells were obtained via direct passage. Then, 1% porcine erythrocyte suspension was prepared using EDTA-treated fresh porcine blood. Viral stock solutions were diluted to 1×10^6 and 1×10^3 TCID₅₀ using autoclaved ddH₂O for parallel beam UV₂₅₄ experiments. A nebulizer aerosolized 15 mL of virus stock solution for each air sampler operation, with a collection duration of 15 min per sampling. Three replications of each experiment were performed. All viral manipulations in cells were conducted at the BSL-3 laboratory of the College of Veterinary Medicine, South China Agricultural University.

2.2 Parallel beam UV experiment

As shown in Figure 1, compared with traditional UV radiometers, the parallel beam apparatus optimizes beam collimation and uniformity, enabling more precise control and measurement of UV₂₅₄ irradiance, thereby enhancing the reliability of experimental results (23). Parallel beam UV₂₅₄ experiments were performed by fixing the UV₂₅₄ illumination of the light source and using different TCID₅₀ values for viruses and varying durations of UV₂₅₄ irradiation. As presented in Supplementary Table S1, the duration of irradiation using the 36-W UV₂₅₄ lamp (wavelength = 254 nm) were set to 0, 3.5, 6.9, 20.8, 34.6, 48.4, 69.2, or 138.4 s, and the UV₂₅₄ dose was set to 0, 0.5, 1, 3, 5, 7, 10, or 20 mJ/cm². After irradiating ASFV (TCID₅₀ = 1×10^6 /CT = 16.45, TCID₅₀ = 1×10^3 /CT = 29.64), PRRSV (TCID₅₀ = 1×10^6 /CT = 14.36, TCID₅₀ = 1×10^3 /CT = 25.36), and PEDV (TCID₅₀ = 1×10^6 /CT = 16.60, TCID₅₀ = 1×10^3 /CT = 27.47), viral inactivation was detected by assessing cytopathic effects (CPEs) and

performing IFAs to determine the UV₂₅₄ dose required for killing effects. Three replications of each experiment were performed.

2.3 Air sterilization experiment

As shown in Figure 2, the air disinfection experiment was performed by adjusting the UV₂₅₄ illumination intensity and wind speed over a fixed UV₂₅₄ irradiation time. The CT values of ASFV, PRRSV, and PEDV stock solutions were 13.5, 12.36, and 11.01, respectively. As illustrated in Supplementary Table S2, the temperature was set to 26°C. Meanwhile, the power of the UV₂₅₄ light (wavelength = 254 nm) was set to 0, 50, or 150 W; the airflow rates in the air sampler and wind tunnel were set to 1 m/s and 2 m/s, respectively, based on the required UV dose. As shown in Figure 3, the corresponding UV₂₅₄ dose was set to 0, 1, 2, 3, 4, or 6 mJ/cm² based on the simulation. First, the air sampler was used to collect airborne particles containing viruses upstream of the sampling section 30 s after nebulization. Subsequently, similar particles were collected downstream. Each collection lasted 15 min to ensure sufficient capture of airborne particles containing viruses. Note that the air sampler must be replaced after each collection, and the downstream sampler should not be connected while the upstream sampler is in operation. The air collected before and after UV₂₅₄ irradiation was dissolved into the culture medium, and viral inactivation was determined by assessing CPEs and performing IFAs. The end of the ventilation duct was equipped with an exhaust gas treatment unit to inhibit the release of viruses into the environment. Three replications of each experiment were performed.

2.4 Nucleic acid extraction and quantitative qPCR

After treatment, nucleic acids were extracted from ASFV, PRRSV, and PEDV using RaPure Viral RNA/DNA Kit (Guangzhou, China) as per the manufacturer's instructions, and qPCR was performed using the reaction system and procedure described previously (24–26). Three assays were performed for each sample. Regarding the results, negative samples had no CT values, positive samples had CT values of ≤34.0 with typical amplification curves, and suspicious samples had CT values of >34.0 with typical amplification curves. If two samples were considered suspicious, the result of the third sample was used.

2.5 Parameters of the parallel beam UV₂₅₄ meter

The impact of UV₂₅₄ light on pathogenic microorganisms is determined by the UV₂₅₄ dose they receive. The UV₂₅₄ is defined as (27):

$$\text{Dose} = \int_0^t I dt$$

where UV₂₅₄ dose is measured in mJ/cm², I represents the UV₂₅₄ light intensity received by the microorganism at a point on its trajectory (mW/cm²), and t is the irradiation time (s). The average UV₂₅₄ intensity received by microorganisms in the water is defined as (28):

TABLE 1 Killing effect of ultraviolet light on viruses.

Virus type	Killing dose	Virus counting (viability) methods	Ultraviolet length	Inactivation rate constant	Medium	Article
Fr bacteriophage	0.5 J/cm ² 99.99 percent reduction	Plaque infectivity test	405		Viral fluid	(18)
ΦX174 bacteriophage	5 J/cm ² 90 percent reduction					
MS2 bacteriophage	679 J/cm ² 99.68 percent reduction	Plaque infectivity test	365–375		Viral fluid	(19)
PhiX-174 bacteriophage	16.1 mJ/cm ² 99.97–99.99 percent reduction	Plaque infectivity test	280		Viral fluid	(20)
MS2 bacteriophage	16.1 mJ/cm ² 99.97–99.99 percent reduction					
MS2 bacteriophage	143.4 mJ/cm ² 99.99–99.9996 percent reduction					
SARS-CoV-2	1.25 mJ/cm ² 90 percent reduction	TCID ₅₀	254	0.79	Water	(30)
	0.6 mJ/cm ² 90 percent reduction	TCID ₅₀	220	1.5		
Adenovirus	10 mJ/cm ² 99.99 percent reduction	qPCR and Plaque infectivity test	210		Water	(51)
	10 mJ/cm ² 99.9 percent reduction		220			
H1N1 influenza virus	10 mJ/cm ² 99.99 percent reduction	IFA	207–222	1.8	Air	(52)
SARS-CoV-2	10 mJ/cm ² 99.99 percent reduction	IFA	254		Air	(53)
SARS-CoV-2	4 mJ/cm ² inactivation 99.9999%	TCID ₅₀	222	12.4	Air	(29)
SARS-CoV-2	2 mJ/cm ² 99.9 percent inactivation	TCID ₅₀ /IFA	222	4.1	Air	(54)
SARS-CoV-2	1,048 mJ/cm ² inactivation 99.999 percent	TCID ₅₀	254		Viral fluid	(55)
SARS-CoV-2	10.25 to 23.71 mJ/cm ² inactivation 99.99 percent	TCID ₅₀	254		Stainless steel, plastic and glass	(56)
SARS-CoV-2	3.7 mJ/cm ² inactivates 99.9 percent	qPCR	254		Water	(57)
SARS-CoV-2	15 mJ/cm ² to inactivate 10 ⁵ TCID ₅₀ virus solution	TCID ₅₀	253.7		Viral fluid	(58)
SARS-CoV-2	0.28 mJ/cm ² 99.2 percent inactivation	qPCR	254		Air	(59)
SARS-CoV-2	10 mJ/cm ₂ inactivation	TCID ₅₀ /IFA	222/230		Water and saliva	(60)
SARS-CoV-2	15 mJ/cm ² 99.99 percent inactivation	TCID ₅₀	222		Viral fluid	(61)
SARS-CoV-2	7.4 mJ/cm ² inactivation	TCID ₅₀	254		—	(62)
SARS-CoV-2	3.6 mJ/cm ² inactivation	Plaque infectivity test	254		Viral fluid	(63)
SARS-CoV-2	3.5 mJ/cm ² inactivation	IFA	254		Viral fluid	(64)

$$E_{ave} = 0.98 \left[\frac{E_0}{L} \left(\frac{(T)^L - 1}{\ln[T]} \right) \right]$$

where E_{ave} represents the average illuminance in the water (mW/cm²), E_0 represents the incident irradiance (mW/cm²), L is the depth of the solution irradiated by the collimated beam (cm), A is the UV₂₅₄ absorbance at a 1-cm light range, and $T = 1 - A$. Considering all irradiated pathogenic microorganisms as a collective group, the total UV₂₅₄ dose received can be calculated as: Dose = $E_{ave} \times t$ (28).

2.6 Air sterilization parameters

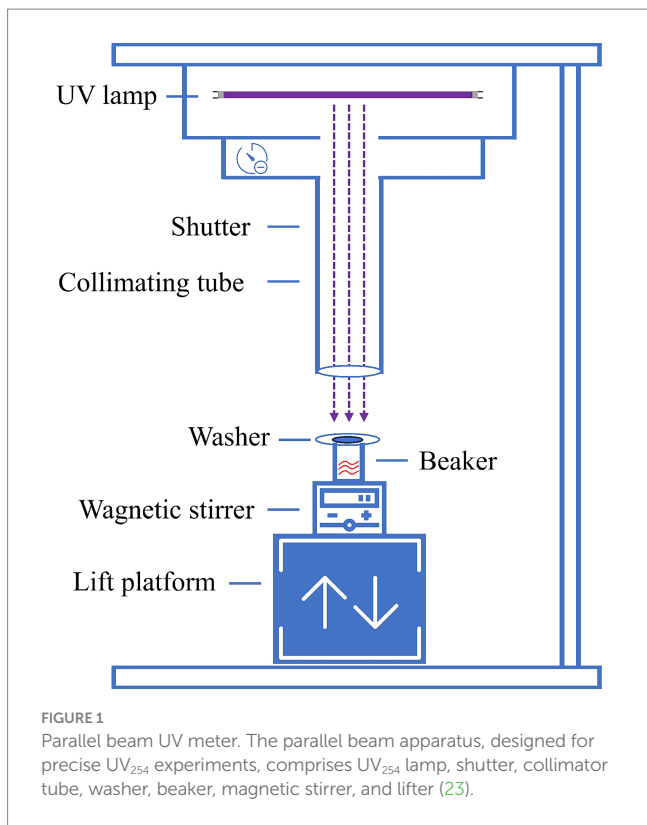
The UV₂₅₄ radiation dose received by a pathogenic microorganism in the reactor is determined by its path and exposure time. The

relationship between microbial inactivation efficiency and UV₂₅₄ dose is defined as (29):

$$-\lg \left(\frac{N}{N_0} \right) = A \times F + B$$

where F is the UV₂₅₄ dose (mJ/cm²); N_0 and N represent the microbial content before and after irradiation, respectively; and A and B are the disinfection kinetic parameters measured using a parallel beam meter. By determining the UV₂₅₄ dose received by each microcluster at the reactor's exit, the corresponding inactivation rate can be calculated. The overall inactivation rate is the combined effect of all microclusters (29):

$$\left(\frac{N}{N_0} \right)_{total} = \frac{\sum 10^{-(A \times F_i + B)}}{T}$$



where F_i represents the UV₂₅₄ dose received by each microcluster at the exit (mJ/cm²) and T is the total number of microclusters. From this, the total effective dose (RED) is defined as (29):

$$RED = - \frac{\left(\lg \left(\frac{N}{N_0} \right)_{total} + B \right)}{A}$$

2.7 Determination of virus infectivity

ASFV samples treated with different UV₂₅₄ doses were used to infect PAMs. Similarly, treated PRRSV samples were used to infect Marc-145 cells, and treated PEDV samples were used to infect Vero cells. Virus infectivity was determined by assessing CPEs and performing IFAs. In brief, PAMs, Marc-145 cells, and Vero cells were inoculated into 96-well plates, and viral suspensions (ASFV diluted in RPMI-1640 containing 10% FBS, PRRSV diluted in Dulbecco’s modified Eagle medium [DMEM] containing 2% FBS, and PEDV diluted in DMEM containing 7 μg/mL trypsin) were added to the plates at a 10-fold gradient (1 × 10⁻¹ to 1 × 10⁻¹⁰), with columns 1 and 12 serving as controls. Viral infectivity was confirmed via the IFA using antibodies specific for ASFV, PRRSV, and PEDV, and the TCID₅₀ was determined using the Reed and Muench method.

2.8 *In vitro* biological characterization of viruses after irradiation

PAMs, Marc-145 cells, and Vero cells were infected with ASFV, PRRSV, and PEDV, respectively, following UV irradiation, and viral

infectivity was confirmed by assessing CPEs and performing IFAs. In brief, PAMs, Marc-145 cells, and Vero cells were inoculated into 96-well plates, and viral suspensions were added to the plates at a 10-fold gradient (1 × 10⁻¹ to 1 × 10⁻¹⁰), with columns 1 and 12 serving as controls. Three replications of each experiment were performed. Viral fluids were collected at 6-h intervals to construct *in vitro* growth curves using GraphPad Prism 8 software (GraphPad, San Diego, CA, United States).

2.9 Data analysis

The UV₂₅₄ dose responses based on UVC at 254 nm were evaluated using a pseudo first-order inactivation kinetics model in the log₁₀ scale as follows (30):

$$\log_{10} I = \log_{10} \left(\frac{N_0}{N} \right) = k \times D$$

where log₁₀ I represents the reduction in infectivity on the log₁₀ scale; N_0 and N represent the infectivity of virus samples before and after UV₂₅₄ exposure, respectively; D represents the UV fluence in mJ/cm²; and k represents the pseudo first-order inactivation rate constant in cm²/mJ computed using a log₁₀-scale kinetic model. The log₁₀ scale inactivation rate constant was used, which facilitated the calculation of log inactivation using the rate constant.

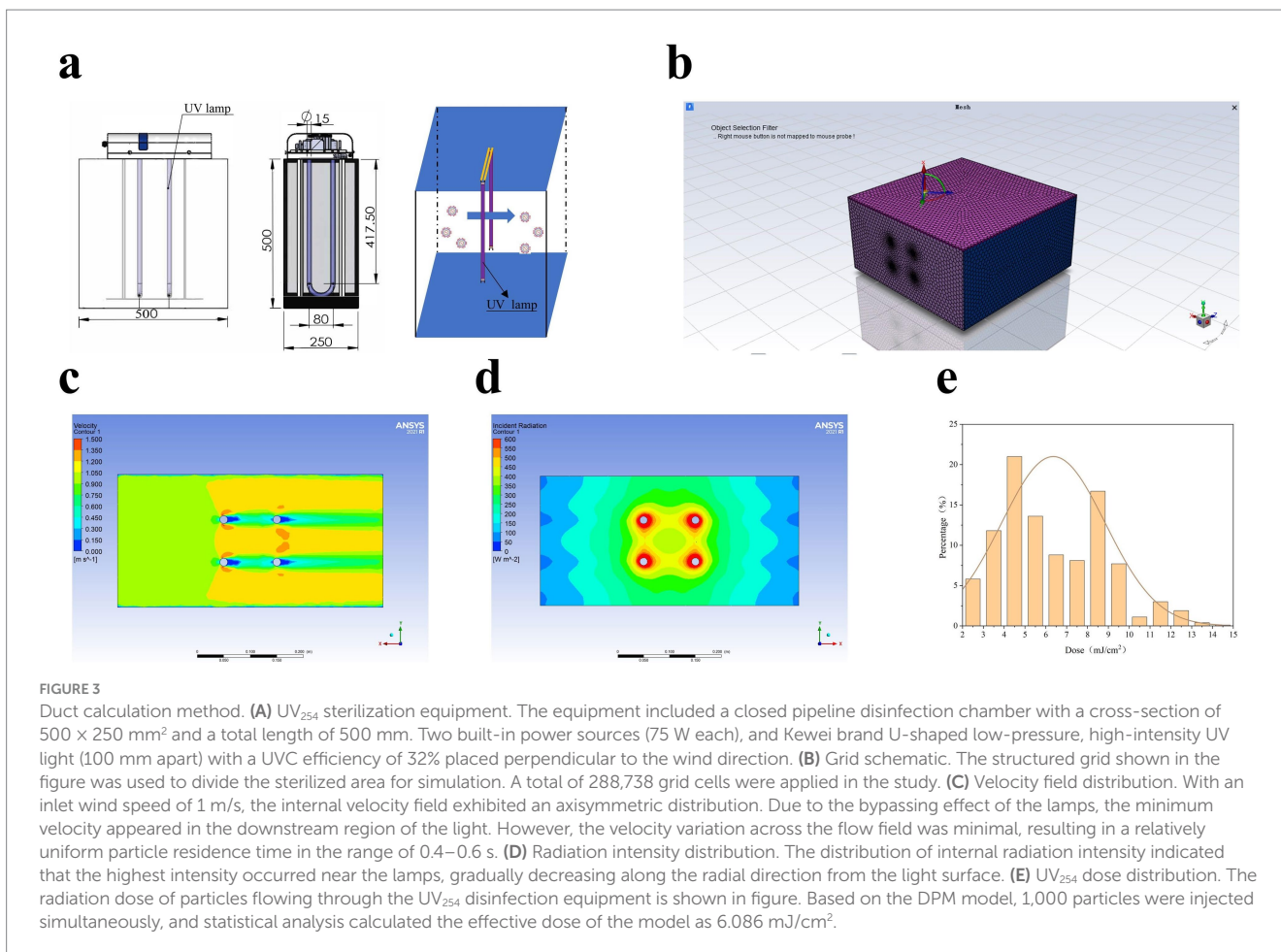
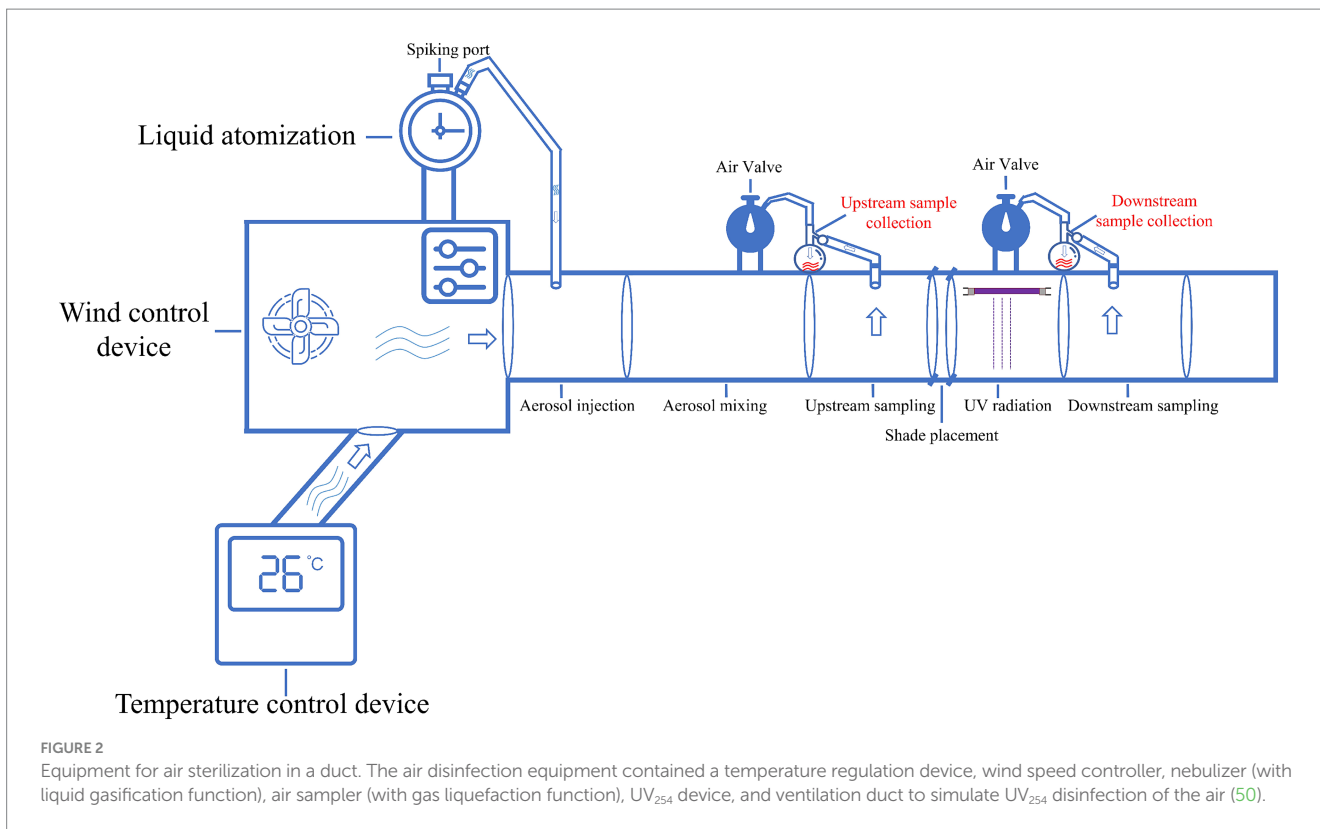
3 Results

3.1 Viral nucleic acids were not degraded by UV₂₅₄ irradiation at different doses

The ASFV, PRRSV, and PEDV solutions were irradiated with different UV₂₅₄ doses (0, 0.5, 1, 3, 5, 7, 10, and 20 mJ/cm²), as presented in Figures 4A–C. The copy numbers of ASFV, PRRSV, and PEDV did not differ significantly among the treatment groups. Further, ASFV, PRRSV, and PEDV were nebulized and then irradiated with different UV₂₅₄ doses (0, 1, 2, 3, and 6 mJ/cm²). As shown in Figure 4D, the copy numbers of the viruses were not altered by nebulization. This suggests that low-dose UV₂₅₄ irradiation does not lead to significant nucleic acid degradation in ASFV, PRRSV, and PEDV.

3.2 Low-dose UV exposure reduces the abundance of infectious virus in the samples

ASFV, PRRSV, and PEDV (TCID₅₀ = 1 × 10⁶) were irradiated at different UV₂₅₄ doses (0, 0.5, 1, 3, 5, 7, 10, and 20 mJ/cm²) and used to infect PAMs, Marc-145 cells, and Vero cells, respectively. As presented in Figure 5A, the fluorescence intensity of ASFV treated with UV₂₅₄ doses of 0.5 and 1 mJ/cm² was significantly lower than that of untreated ASFV, and no fluorescence was observed for ASFV treated with an external UV₂₅₄ dose of 3 mJ/cm². The fluorescence intensity of PRRSV treated with a UV₂₅₄ dose of 0.5 mJ/cm² was significantly lower than that of untreated PRRSV, and no fluorescence was observed for PRRSV treated with an external UV₂₅₄ dose of 1 mJ/cm². The fluorescence intensity of PEDV treated with a UV₂₅₄ dose of 0.5 mJ/cm² was



significantly lower than that of untreated PEDV, and no fluorescence was observed for PEDV treated with an external UV₂₅₄ dose of 1 mJ/cm². As shown in Figures 5B–D, the infectivity of the viruses decreased significantly with increasing UV₂₅₄ doses, and ASFV was more resistant to UV₂₅₄ irradiation than PRRSV and PEDV. These results indicated that low-dose UV₂₅₄ irradiation can reduce the infectivity of viruses in cells.

3.3 Quantification of UV₂₅₄-induced inactivation of ASFV, PRRSV, and PEDV

Water and air containing ASFV, PRRSV, and PEDV were irradiated with different doses of UV₂₅₄ and were subsequently used to infect PAMs, Marc-145 cells, and Vero cells, respectively. Figure 6A, linear regression analysis revealed a rate constant of 4.308 cm²/mJ (95% confidence interval = 3.943–4.674) for ASFV, which corresponds to a 90% inactivation dose (D₉₀) of 0.23 mJ/cm². In addition, the rate constant for PRRSV was 9.167 cm²/mJ (95% confidence interval = 8.704–9.629), which corresponds to a D₉₀ of 0.11 mJ/cm². Further, the rate constant for PEDV was 8.333 cm²/mJ (95% confidence interval = 7.871–8.796), corresponding to a D₉₀ of 0.12 mJ/cm². Figure 6B, linear regression analysis revealed a rate constant of 3.167 cm²/mJ (95% confidence interval = 2.461–3.872) for ASFV, which corresponds to a 90% inactivation dose (D₉₀) of 0.32 mJ/cm². In addition, the rate constant for PRRSV was 2.958 cm²/mJ (95% confidence interval = 1.985–3.932), which corresponds to a D₉₀ of 0.338 mJ/cm². Further, the rate constant for PEDV was

2.538 cm²/mJ (95% confidence interval = 1.396–3.681), corresponding to a D₉₀ of 0.394 mJ/cm².

3.4 UV₂₅₄ doses exceeding 1 mJ/cm² inactivate ASFV, PRRSV, and PEDV in the air

ASFV, PRRSV, and PEDV were collected through an air sampler after irradiation with different UV₂₅₄ doses (0, 1, 2, 3, and 6 mJ/cm²) and used to infect PAMs, Marc-145 cells, and Vero cells, respectively. As presented in Figure 7, ASFV, PRRSV, and PEDV irradiated with a UV₂₅₄ dose of 1 mJ/cm² lost the ability to infect cells, whereas untreated viruses caused obvious lesions in the cells within 48 h after inoculation. The IFA and growth curves indicated that the untreated viruses showed normal replication in the cells.

4 Discussion

The ASF outbreak in China in August 2018 led to major changes in pig farming patterns in China, including the introduction of biosecurity prevention and control (31, 32). Previous studies have revealed that the positivity rates of various swine diseases decreased significantly with the establishment of biosecurity prevention and control systems in Chinese pig farms (33). Disinfection is an important part of the biosafety system (34). Currently, chemical disinfection is commonly used in pig farms because of its ease of use and obvious inactivate effects against pathogenic microorganisms

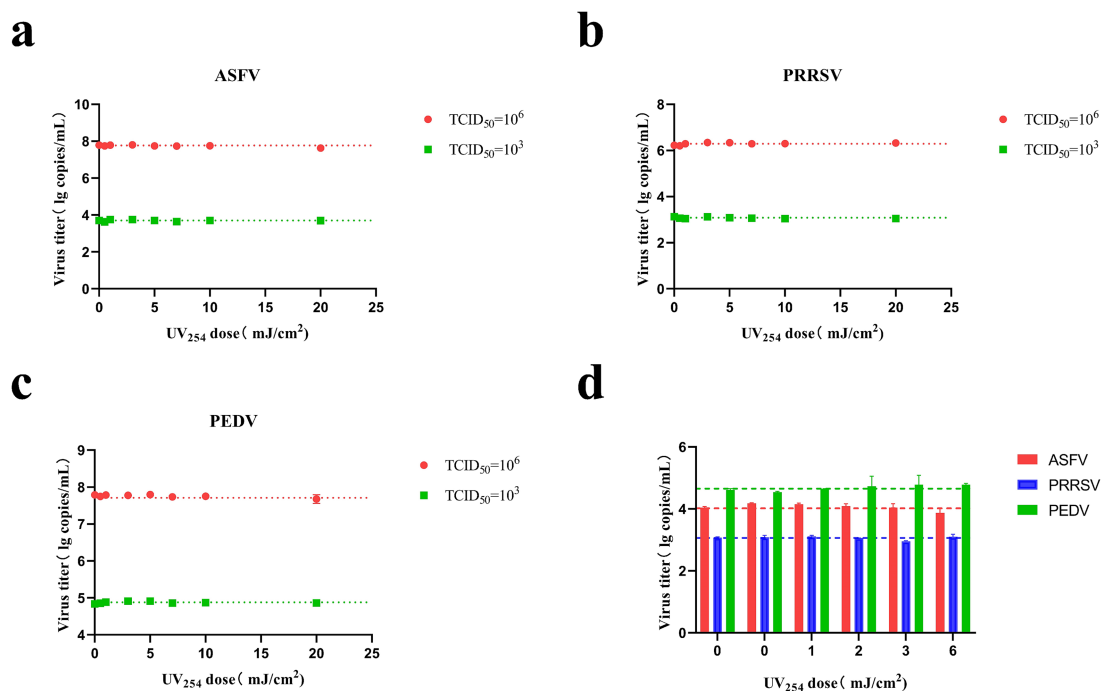


FIGURE 4

Changes in the CT values of ASFV, PRRSV, and PEDV after irradiation with different UV doses. (A) Irradiation of ASFV solution (TCID₅₀ = 1 × 10⁶ and 1 × 10³) using a parallel beam UV device. (B) Irradiation of PRRSV solution (TCID₅₀ = 1 × 10³ and 1 × 10⁶) using a parallel beam UV device. (C) Irradiation of PEDV solution (TCID₅₀ = 1 × 10³ and 1 × 10⁶) using a parallel beam UV device. (D) Irradiation of aerosolized ASFV, PRRSV, and PEDV in air disinfection ducts.

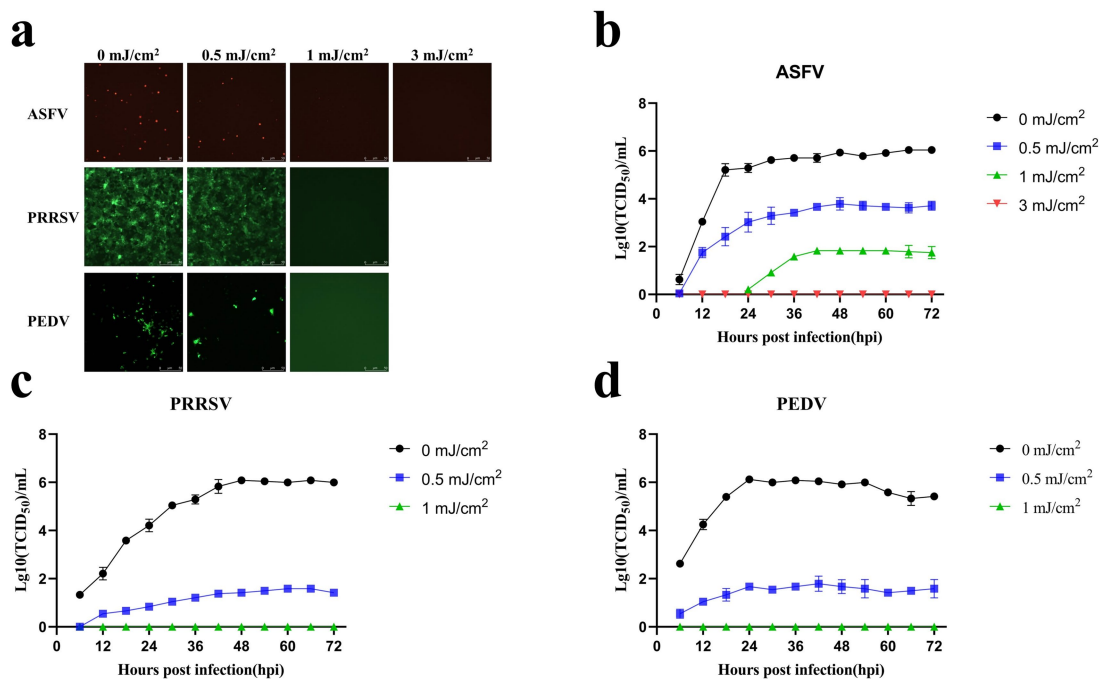


FIGURE 5

Low-dose UV₂₅₄ irradiation reduces the abundance of infectious virus in the samples. (A) Changes in the fluorescence signals of ASFV, PRRSV, and PEDV after treatment with different UV doses. (B) Growth curves of ASFV after treatment with different UV₂₅₄ doses. (C) Growth curves of PRRSV after treatment with different UV₂₅₄ doses. (D) Growth curves of PEDV after treatment with different UV₂₅₄ doses.

(35, 36). However, this disinfection method is associated with various problems, such as the presence of residual chemicals, secondary pollution, and formation of toxic disinfection by-products (DBPs). In addition, the types and usage of disinfectants applied on different objects are diverse, and some disinfectants are prone to cause damage to feed, food, and electronics. Therefore, chemical disinfection methods cannot be used in all scenarios in pig farms (37–42).

UV₂₅₄ treatment is a physical disinfection method, and the use of the UVC band for UV₂₅₄ irradiation leads to photochemical damage and ROS generation in pathogenic microorganisms, which affects the replication and transcription of genetic material and cause cell membrane and cell wall damage, ultimately leading to the death of microorganisms (13, 14, 27, 38, 43). Compared with chemical disinfection, UV₂₅₄ disinfection is characterized by short disinfection time, high efficiency, broad germicidal spectrum, simple structure, small footprint, easy maintenance, and the absence of DBP production, resulting in its widespread use in multiple applications, such as air disinfection, water purification and wastewater treatment, food preservation, and medical applications (11, 12, 44, 45). The effectiveness of UV-mediated inactivation depends on the type of pathogenic microorganism and operating conditions, such as UV wavelength, UV intensity, and duration of irradiation. Moreover, environmental conditions can also affect the efficacy of UV-based inactivation (11, 46).

ASFV, PRRSV, and PEDV are the three most serious viral diseases that can be transmitted through the air to pig farms in China. Similar to SARS-CoV-2 in humans, these viruses can cause widespread and rapid damage in infected pigs if their spread is not controlled, as observed during the ASF outbreak in China in 2018 (31, 47–49). It is

well known that UV₂₅₄ treatment has a strong killing effect. Currently, although UV₂₅₄ disinfection is widely used in pig farms, research on its killing effects on these three viruses is less extensive than that on SARS-CoV-2. Water and air are two important media for viral transmission. In the early stage of experimental designing, we reviewed a large number of studies on the killing effects of UV₂₅₄ disinfection. We revealed that UV₂₅₄ treatment has a stronger effect on viruses in the air than in viruses in the water. A UV₂₅₄ dose of <1 mJ/cm² can inactivate 99.9% of SARS-CoV-2 virions, and the killing effect of UV₂₅₄ is stronger in pure water than in culture medium. Compared with other wavelengths, UV₂₅₄ irradiation at a wavelength of 254 nm has a stronger killing effect (31, 47–49).

We investigated the UV₂₅₄ dose required to inactivate ASFV, PRRSV, and PEDV in pure water using a UV₂₅₄ parallel beam meter and then assessed its effects on viruses in the air using air sterilization equipment. We used primers and probes specific to ASFV-B646L, PRRSV-ORF6, and PEDV-M genes to detect the viral nucleic acid abundance of ASFV, PRRSV, and PEDV, respectively, before and after irradiation with different UV₂₅₄ doses (parallel beam UV₂₅₄ system: 0–20 mJ/cm²; air sterilization duct: 0–6 mJ/cm²). Further, we assessed viral infectivity by measuring CPEs and performing IFAs. The results revealed that low-dose UV₂₅₄ irradiation did not significantly degrade viral nucleic acids or suppress viral infectivity. In addition, ASFV, PRRSV, and PEDV treated with UV₂₅₄ doses of 3, 1, and 1 mJ/cm², respectively, these viral fluids were found to be infectivity-incompetent. To more intuitively demonstrate the relationship of the UV₂₅₄ dose with ASFV, PRRSV, and PEDV inactivation, the inactivation rate was quantified as the ratio of TCID₅₀ before and after UV irradiation. ASFV was more resistant to UV₂₅₄ irradiation than PRRSV and PEDV, probably because ASFV consists of a four-layered

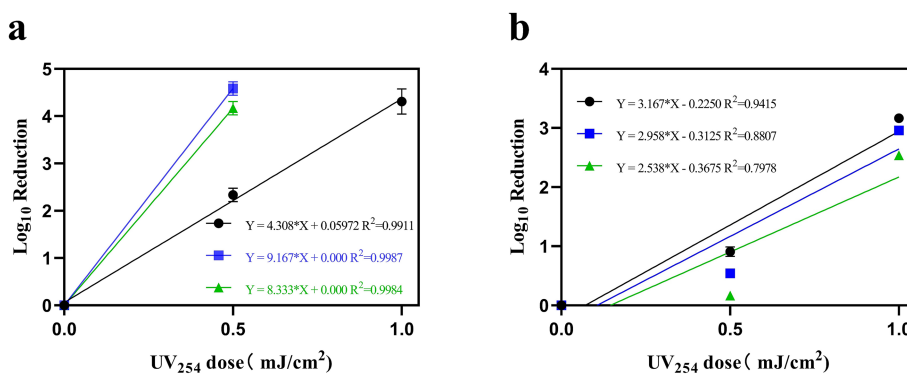


FIGURE 6 The relationship between the inactivation of ASFV, PRRSV, and PEDV in water (A) and air (B) with UV₂₅₄ dose, measured by TCID₅₀ relative to untreated virus controls. (Black indicates ASFV; blue indicates PRRSV; and green indicates PEDV).

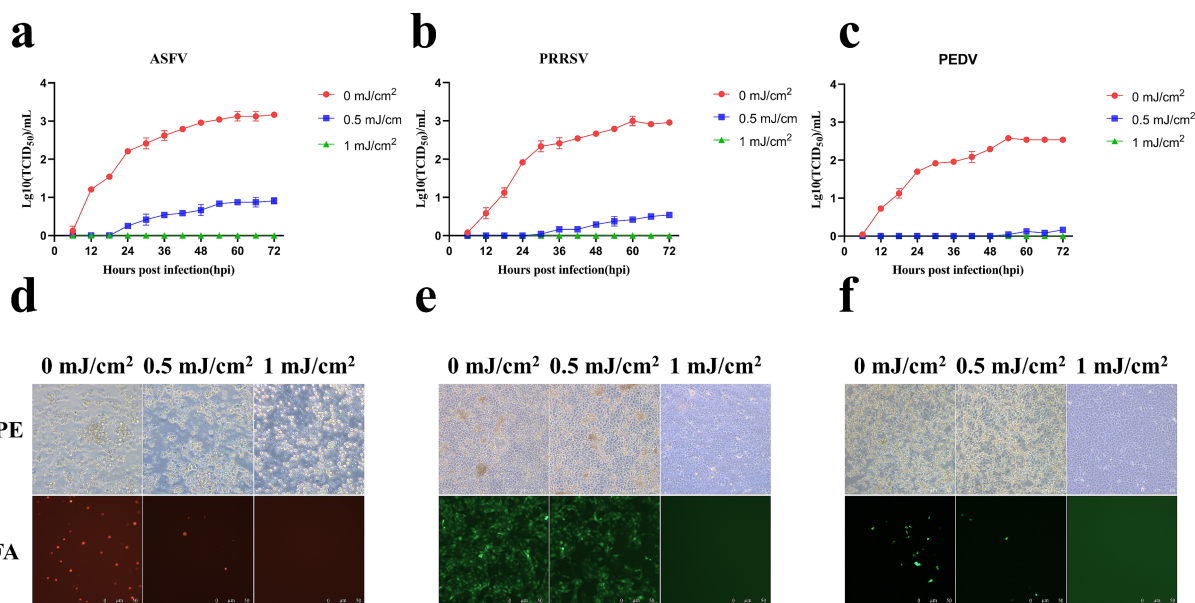


FIGURE 7 Replication of ASFV, PRRSV, and PEDV after UV₂₅₄ treatment at a dose of 1 mJ/cm². (A–C) Growth curves of ASFV, PRRSV, and PEDV. (D–F) CPEs and IFA data for ASFV, PRRSV, and PEDV.

protein shell and an internal genome, which is apparently more complex in structure than the internal genomes of PRRSV and PEDV. The air sterilization experiment revealed good cell growth, no cell lesions, and no fluorescence in the 1 mJ/cm² treatment group, suggesting that this dose is sufficient to inactivate ASFV, PRRSV, and PEDV. The stronger killing effects of UV₂₅₄ in the air than in the water are likely attributable to the fact that UV₂₅₄ can directly contact viruses in the air, whereas water refracts UV₂₅₄ light. This experiment was performed under ideal conditions where in UV₂₅₄ irradiation was applied directly to the viruses, resulting in killing effects at low doses. In real-world situations, the environment is intricate, and the number and size of dust particles in water and air can affect the efficiency of UV₂₅₄ disinfection. Therefore, it may be necessary to increase the UV dose in practical applications. In summary, we believe that UV₂₅₄

disinfection can be used in air filtration devices and other joint applications to detoxify air.

5 Conclusion

This study revealed that low-dose (0–20 mJ/cm²) UV₂₅₄ irradiation significantly reduces viral infectivity without causing nucleic acid degradation. Using parallel beam UV₂₅₄ apparatus, the UV₂₅₄ doses required to inactivate ASFV, PRRSV, and PEDV were preliminarily determined to be 3, 1, and 1 mJ/cm², respectively. The air disinfection experiment illustrated that a UV₂₅₄ dose of 1 mJ/cm² was sufficient to eradicate ASFV, PRRSV, and PEDV. These findings may provide a reference for the design and application of UV₂₅₄ equipment in pig

farms and lay a foundation for further research and development regarding viral disinfection.

Data availability statement

The original contributions presented in the study are included in the article/[Supplementary material](#), further inquiries can be directed to the corresponding authors.

Author contributions

YQ: Conceptualization, Writing – original draft, Software. QL: Resources, Software, Writing – review & editing. WZ: Data curation, Supervision, Writing – review & editing. HC: Project administration, Validation, Writing – review & editing. JW: Supervision, Validation, Writing – review & editing. QG: Supervision, Visualization, Writing – review & editing. QZ: Formal analysis, Resources, Visualization, Writing – review & editing. GZ: Formal analysis, Project administration, Writing – review & editing. LG: Conceptualization, Data curation, Writing – original draft. LW: Conceptualization, Validation, Writing – review & editing.

Funding

The author(s) declare that financial support was received for the research, authorship, and/or publication of this article. This research was funded by the National Key Research and Development Program of China (2021YFD1800100), the Start-Up Research Project of Maoming Laboratory (2021TDQD002), and the China Agriculture Research System of MOF and MARA (CARS-35), Postdoctoral Fellowship Program of CPSF (GZC20230860).

References

- Tong B, Zhang L, Hou Y, Oenema O, Long W, Velthof G, et al. Lower pork consumption and technological change in feed production can reduce the pork supply chain environmental footprint in China. *Nat Food*. (2023) 4:74–83. doi: 10.1038/s43016-022-00640-6
- Gaudreault NN, Madden DW, Wilson WC, Trujillo JD, Richt JA. African swine fever virus: an emerging DNA arbovirus. *Front Vet Sci*. (2020) 7:215. doi: 10.3389/fvets.2020.00215
- VanderWaal K, Deen J. Global trends in infectious diseases of swine. *Proc Natl Acad Sci USA*. (2018) 115:11495–500. doi: 10.1073/pnas.1806068115
- Yang H, Zhou L. Epidemic situation of swine diseases in 2022 and trends and prevention strategies for 2023. *Swine Ind Sci*. (2023) 40:58–60. doi: 10.3969/j.issn.1673-5358.2023.02.018
- Blome S, Franke K, Beer M. African swine fever—a review of current knowledge. *Virus Res*. (2020) 287:198099. doi: 10.1016/j.virusres.2020.198099
- Guinat C, Gogin A, Blome S, Keil G, Pollin R, Pfeiffer DU, et al. Transmission routes of African swine fever virus to domestic pigs: current knowledge and future research directions. *Vet Rec*. (2016) 178:262–7. doi: 10.1136/vr.103593
- Olesen AS, Lohse L, Boklund A, Halasa T, Gallardo C, Pejsak Z, et al. Transmission of African swine fever virus from infected pigs by direct contact and aerosol routes. *Vet Microbiol*. (2017) 211:92–102. doi: 10.1016/j.vetmic.2017.10.004
- Arruda AG, Tousignant S, Sanhueza J, Vilalta C, Poljak Z, Torremorell M, et al. Aerosol detection and transmission of porcine reproductive and respiratory syndrome virus (PRRSV): what is the evidence, and what are the knowledge gaps? *Viruses*. (2019) 11:712. doi: 10.3390/v11080712
- Alonso C, Goede DP, Morrison RB, Davies PR, Rovira A, Marthaler DG, et al. Evidence of infectivity of airborne porcine epidemic diarrhea virus and detection of

Acknowledgments

The authors thank Qi Gao, HeYou Yi, and Yu Wu for providing qPCR primers and probes.

Conflict of interest

JW was employed by Foshan Comwin Light & Electricity Co., Ltd. The remaining authors declare that the research was conducted in the absence of any commercial or financial relationships that could be construed as a potential conflict of interest.

Generative AI statement

The authors declare that no Generative AI was used in the creation of this manuscript.

Publisher's note

All claims expressed in this article are solely those of the authors and do not necessarily represent those of their affiliated organizations, or those of the publisher, the editors and the reviewers. Any product that may be evaluated in this article, or claim that may be made by its manufacturer, is not guaranteed or endorsed by the publisher.

Supplementary material

The Supplementary material for this article can be found online at: <https://www.frontiersin.org/articles/10.3389/fvets.2025.1512387/full#supplementary-material>

airborne viral RNA at long distances from infected herds. *Vet Res*. (2014) 45:73. doi: 10.1186/s13567-014-0073-z

10. Li X, Hu Z, Fan M, Tian X, Wu W, Gao W, et al. Evidence of aerosol transmission of African swine fever virus between two piggeries under field conditions: a case study. *Front Vet Sci*. (2023) 10:1201503. doi: 10.3389/fvets.2023.1201503

11. Li X, Cai M, Wang L, Niu F, Yang D, Zhang G. Evaluation survey of microbial disinfection methods in UV-LED water treatment systems. *Sci Total Environ*. (2019) 659:1415–27. doi: 10.1016/j.scitotenv.2018.12.344

12. Bono N, Ponti F, Punta C, Candiani G. Effect of UV irradiation and TiO₂-photocatalysis on airborne bacteria and viruses: an overview. *Materials*. (2021) 14:1075. doi: 10.3390/ma14051075

13. Song K, Taghipour F, Mohseni M. Microorganisms inactivation by wavelength combinations of ultraviolet light-emitting diodes (UV-LEDs). *Sci Total Environ*. (2019) 665:1103–10. doi: 10.1016/j.scitotenv.2019.02.041

14. Martin-Somer M, Pablos C, Adan C, van Grieken R, Marugan J. A review on LED technology in water photodisinfection. *Sci Total Environ*. (2023) 885:163963. doi: 10.1016/j.scitotenv.2023.163963

15. Misstear DB, Gill LW. The inactivation of phages MS2, ΦX174 and PR772 using UV and solar photocatalysis. *J Photochem Photobiol B*. (2012) 107:1–8. doi: 10.1016/j.jphotobiol.2011.10.012

16. Hull NM, Linden KG. Synergy of MS2 disinfection by sequential exposure to tailored UV wavelengths. *Water Res*. (2018) 143:292–300. doi: 10.1016/j.watres.2018.06.017

17. Darnell ME, Subbarao K, Feinstone SM, Taylor DR. Inactivation of the coronavirus that induces severe acute respiratory syndrome, SARS-CoV. *J Virol Methods*. (2004) 121:85–91. doi: 10.1016/j.jviromet.2004.06.006

18. Heffron J, Bork M, Mayer BK, Skwor T. A comparison of porphyrin photosensitizers in photodynamic inactivation of RNA and DNA bacteriophages. *Viruses*. (2021) 13:530. doi: 10.3390/v13030530
19. Spunde K, Rudevica Z, Korotkaja K, Skudra A, Gudermanis R, Zajakina A, et al. Bacteria and RNA virus inactivation with a high-irradiance UV-A source. *Photochem Photobiol Sci*. (2024) 23:1841–56. doi: 10.1007/s43630-024-00634-2
20. Freitas BLS, Fava NMDN, Melo-Neto MGD, Dalkiranis GG, Tonetti AL, Byrne JA, et al. Efficacy of UVC-LED radiation in bacterial, viral, and protozoan inactivation: an assessment of the influence of exposure doses and water quality. *Water Res*. (2024) 266:122322. doi: 10.1016/j.watres.2024.122322
21. Jing Z, Wang W, Nong Y, Peng L, Yang Z, Ye B, et al. Suppression of photoreactivation of *E. coli* by excimer far-UV light (222 nm) via damage to multiple targets. *Water Res*. (2024) 255:121533. doi: 10.1016/j.watres.2024.121533
22. Yu M, Gao R, Lv X, Sui M, Li T. Inactivation of phage phiX174 by UV₂₅₄ and free chlorine: structure impairment and function loss. *J Environ Manage*. (2023) 340:117962. doi: 10.1016/j.jenvman.2023.117962
23. Qiang Z, Li W, Li M, Bolton JR, Qu J. Inspection of feasible calibration conditions for UV radiometer detectors with the KI/KIO₃ actinometer. *Photochem Photobiol*. (2015) 91:68–73. doi: 10.1111/php.12356
24. Gao Q, Feng Y, Yang Y, Luo Y, Gong T, Wang H, et al. Establishment of a dual real-time PCR assay for the identification of African swine fever virus genotypes I and II in China. *Front Vet Sci*. (2022) 9:882824. doi: 10.3389/fvets.2022.882824
25. Yi H, Yu Z, Wang Q, Sun Y, Peng J, Cai Y, et al. *Panax notoginseng* saponins suppress type 2 porcine reproductive and respiratory syndrome virus replication *in vitro* and enhance the immune effect of the live vaccine JXA1-R in piglets. *Front Vet Sci*. (2022) 9:886058. doi: 10.3389/fvets.2022.886058
26. Wu Y, Li W, Zhou Q, Li Q, Xu Z, Shen H, et al. Characterization and pathogenicity of Vero cell-attenuated porcine epidemic diarrhea virus CT strain. *Virol J*. (2019) 16:121. doi: 10.1186/s12985-019-1232-7
27. Han X. Design and process parameter optimization of ultraviolet disinfection devices. Changchun: Jilin Agricultural University (2006).
28. Freeman S, Kibler K, Lipsky Z, Jin S, German GK, Ye K. Systematic evaluating and modeling of SARS-CoV-2 UVC disinfection. *Sci Rep*. (2022) 12:5869. doi: 10.1038/s41598-022-09930-2
29. Welch D, Buonanno M, Buchan AG, Yang L, Atkinson KD, Shuryak I, et al. Inactivation rates for airborne human coronavirus by low doses of 222 nm far-UVC radiation. *Viruses*. (2022) 14:684. doi: 10.3390/v14040684
30. Ma B, Gundy PM, Gerba CP, Sobsey MD, Linden KG. UV inactivation of SARS-CoV-2 across the UVC spectrum: KrCl⁺ excimer, mercury-vapor, and light-emitting-diode (LED) sources. *Appl Environ Microbiol*. (2021) 87:e0153221. doi: 10.1128/AEM.01532-21
31. Gao L, Sun X, Yang H, Xu Q, Li J, Kang J, et al. Epidemic situation and control measures of African swine fever outbreaks in China 2018–2020. *Transbound Emerg Dis*. (2021) 68:2676–86. doi: 10.1111/tbed.13968
32. Chen H, Liu X, Li C. Epidemiological characteristics and prevention and control of major swine diseases in China. *Swine Ind Today*. (2022) 2:8–15.
33. Wang Y, Song D, Zhao M, Yan R, Ban F. Exploring new strategies for swine disease prevention and control based on the detection of swine diseases before and after the outbreak of African swine fever. *Mod Anim Husband*. (2022) 6:41–5.
34. Liu Y, Zhang X, Qi W, Yang Y, Liu Z, An T, et al. Prevention and control strategies of African swine fever and progress on pig farm repopulation in China. *Viruses*. (2021) 13:2552. doi: 10.3390/v13122552
35. Beato MS, D'Errico F, Iscaro C, Petrini S, Giammaroli M, Feliziani F. Disinfectants against African swine fever: an updated review. *Viruses*. (2022) 14:1384. doi: 10.3390/v14071384
36. Ni Z, Chen L, Yun T, Xie R, Ye W, Hua J, et al. Inactivation performance of pseudorabies virus as African swine fever virus surrogate by four commercialized disinfectants. *Vaccines*. (2023) 11:579. doi: 10.3390/vaccines11030579
37. Sun X, Chen M, Wei D, Du Y. Research progress of disinfection and disinfection by-products in China. *J Environ Sci*. (2019) 81:52–67. doi: 10.1016/j.jes.2019.02.003
38. Zhao C, Fan S, Du X, Deng Q, Liu C. Research progress on ultraviolet disinfection technology in pig farms. *China Anim Health Insp*. (2021) 38:88–94. doi: 10.3969/j.issn.1005
39. Leclercq L, Nardello-Rataj V. How to improve the chemical disinfection of contaminated surfaces by viruses, bacteria and fungus? *Eur J Pharm Sci*. (2020) 155:105559. doi: 10.1016/j.ejps.2020.105559
40. Farre MJ, Day S, Neale PA, Stalter D, Tang JY, Escher BI. Bioanalytical and chemical assessment of the disinfection by-product formation potential: role of organic matter. *Water Res*. (2013) 47:5409–21. doi: 10.1016/j.watres.2013.06.017
41. Deleo PC, Huynh C, Pattanayek M, Schmid KC, Pechacek N. Assessment of ecological hazards and environmental fate of disinfectant quaternary ammonium compounds. *Ecotoxicol Environ Saf*. (2020) 206:111116. doi: 10.1016/j.ecoenv.2020.111116
42. Qin J, Xia PF, Yuan XZ, Wang SG. Chlorine disinfection elevates the toxicity of polystyrene microplastics to human cells by inducing mitochondria-dependent apoptosis. *J Hazard Mater*. (2022) 425:127842. doi: 10.1016/j.jhazmat.2021.127842
43. Besaratinia A, Yoon JI, Schroeder C, Bradforth SE, Cockburn M, Pfeifer GP. Wavelength dependence of ultraviolet radiation-induced DNA damage as determined by laser irradiation suggests that cyclobutane pyrimidine dimers are the principal DNA lesions produced by terrestrial sunlight. *FASEB J*. (2011) 25:3079–91. doi: 10.1096/fj.11-187336
44. Kebbi Y, Muhammad AI, Sant'Ana AS, Do PL, Liu D, Ding T. Recent advances on the application of UV-LED technology for microbial inactivation: progress and mechanism. *Compr Rev Food Sci Food Saf*. (2020) 19:3501–27. doi: 10.1111/1541-4337.12645
45. Song K, Mohseni M, Taghipour F. Application of ultraviolet light-emitting diodes (UV-LEDs) for water disinfection: a review. *Water Res*. (2016) 94:341–9. doi: 10.1016/j.watres.2016.03.003
46. Laghari AA, Liu L, Kalhoro DH, Chen H, Wang C. Mechanism for reducing the horizontal transfer risk of the airborne antibiotic-resistant genes of *Escherichia coli* species through microwave or UV irradiation. *Int J Environ Res Public Health*. (2022) 19:4332. doi: 10.3390/ijerph19074332
47. Synowiec A, Szczepanski A, Barreto-Duran E, Lie LK, Pyrc K. Severe acute respiratory syndrome coronavirus 2 (SARS-CoV-2): a systemic infection. *Clin Microbiol Rev*. (2021) 34:e00133. doi: 10.1128/CMR.00133-20
48. Du T, Nan Y, Xiao S, Zhao Q, Zhou EM. Antiviral strategies against PRRSV infection. *Trends Microbiol*. (2017) 25:968–79. doi: 10.1016/j.tim.2017.06.001
49. Zhang H, Zou C, Peng O, Ashraf U, Xu Q, Gong L, et al. Global dynamics of porcine enteric coronavirus PEDV epidemiology, evolution, and transmission. *Mol Biol Evol*. (2023) 40:msad052. doi: 10.1093/molbev/msad052
50. Wang Y ed. Research on dynamic ultraviolet irradiation air disinfection technology in air ducts. Tianjin: Tianjin University (2012).
51. Beck SE, Rodriguez RA, Linden KG, Hargy TM, Larason TC, Wright HB. Wavelength dependent UV inactivation and DNA damage of adenovirus as measured by cell culture infectivity and long range quantitative PCR. *Environ Sci Technol*. (2014) 48:591–8. doi: 10.1021/es403850b
52. Welch D, Buonanno M, Grilj V, Shuryak I, Crickmore C, Bigelow AW, et al. Far-UVC light: a new tool to control the spread of airborne-mediated microbial diseases. *Sci Rep*. (2018) 8:2752. doi: 10.1038/s41598-018-21058-w
53. Ruetalo N, Berger S, Niessner J, Schindler M. Inactivation of aerosolized SARS-CoV-2 by 254 nm UV-C irradiation. *Indoor Air*. (2022) 32:e13115. doi: 10.1111/ina.13115
54. Buonanno M, Welch D, Shuryak I, Brenner DJ. Far-UVC light (222 nm) efficiently and safely inactivates airborne human coronaviruses. *Sci Rep*. (2020) 10:10285. doi: 10.1038/s41598-020-67211-2
55. Heilingloh CS, Aufderhorst UW, Schipper L, Dittmer U, Witzke O, Yang D, et al. Susceptibility of SARS-CoV-2 to UV irradiation. *Am J Infect Control*. (2020) 48:1273–5. doi: 10.1016/j.ajic.2020.07.031
56. Gidari A, Sabbatini S, Bastianelli S, Pierucci S, Busti C, Bartolini D, et al. SARS-CoV-2 survival on surfaces and the effect of UV-C light. *Viruses*. (2021) 13:408. doi: 10.3390/v13030408
57. Biasin M, Bianco A, Pareschi G, Cavalleri A, Cavatorta C, Fenizia C, et al. UV-C irradiation is highly effective in inactivating SARS-CoV-2 replication. *Sci Rep*. (2021) 11:6260. doi: 10.1038/s41598-021-85425-w
58. Lo CW, Matsuura R, Iimura K, Wada S, Shinjo A, Benno Y, et al. UVC disinfects SARS-CoV-2 by induction of viral genome damage without apparent effects on viral morphology and proteins. *Sci Rep*. (2021) 11:13804. doi: 10.1038/s41598-021-93231-7
59. Garg H, Ringe RP, Das S, Parkash S, Thakur B, Delipan R, et al. UVC-based air disinfection systems for rapid inactivation of SARS-CoV-2 present in the air. *Pathogens*. (2023) 12:419. doi: 10.3390/pathogens12030419
60. Schuit MA, Larason TC, Krause ML, Green BM, Holland BP, Wood SP, et al. SARS-CoV-2 inactivation by ultraviolet radiation and visible light is dependent on wavelength and sample matrix. *J Photochem Photobiol B*. (2022) 233:112503. doi: 10.1016/j.jphotobiol.2022.112503
61. Kitagawa H, Nomura T, Nazmul T, Kawano R, Omori K, Shigemoto N, et al. Effect of intermittent irradiation and fluence-response of 222 nm ultraviolet light on SARS-CoV-2 contamination. *Photodiagn Photodyn Ther*. (2021) 33:102184. doi: 10.1016/j.pdpdt.2021.102184
62. Maquart M, Marlet J. Rapid SARS-CoV-2 inactivation by mercury and led UV-C lamps on different surfaces. *Photochem Photobiol Sci*. (2022) 21:2243–7. doi: 10.1007/s43630-022-00292-2
63. Storm N, McKay L, Downs SN, Johnson RI, Birru D, de Samber M, et al. Rapid and complete inactivation of SARS-CoV-2 by ultraviolet-C irradiation. *Sci Rep*. (2020) 10:22421. doi: 10.1038/s41598-020-79600-8
64. Ruetalo N, Businger R, Schindler M. Rapid, dose-dependent and efficient inactivation of surface dried SARS-CoV-2 by 254 nm UV-C irradiation. *Euro Surveill*. (2021) 26:2001718. doi: 10.2807/1560-7917.ES.2021.26.42.2001718